

# Remote Sensing and Artificial Neural Network Estimation of On-Road Vehicle Emissions

Zerui Li, Yu Kang, Wenjun Lv

Department of Automation  
University of Science and Technology of China  
Hefei, 230022, China

Email: {lzerui,lvwenjun}@mail.ustc.edu.cn,kangduyu@ustc.edu.cn,

Yunbo Zhao

College of Information Engineering  
Zhejiang University of Technology  
Hangzhou, 310023, China

Email: ybzhao@zjut.edu.cn

**Abstract**—The emissions of on-road vehicles are studied based on a remote sensing system and artificial neural network models. A transportable vehicle emission remote sensing system is used to collect the emission data from May to August 2012 in Hefei, China. Based on these light-duty gasoline vehicle data containing the emission pollutants such as carbon monoxide, hydrocarbons, nitric oxide, and so on, artificial neural network models are constructed to estimate the relation of fuel-based emission factors and input parameters. The performance of the developed models is analyzed and compared, showing that neural networks perform better than the multiple linear regression models, thus validating the effectiveness of neural networks in vehicle emission estimation.

## I. INTRODUCTION

Motor vehicle emissions are a major contributor to urban air pollution, causing serious adverse effects on the environment and human health. To estimate gas components in vehicle emissions under various meteorological conditions and driving patterns, is therefore becoming one key problem in order to improve urban air quality.

A widely used method to estimate emissions of vehicles is the chassis and engine dynamometer testing. It has good precision, repeatability, and is economical, but simulated driving patterns are simply not real-world conditions [1]. Another method, the tunnel studies measure the air flow through a tunnel, and the difference in gas concentrations of outlet and inlet can represent emissions of vehicle. This method can be closer to the real-world conditions than the dynamometer test, but it can not provide instantaneous emission status of vehicles. The results are only the average emission status [2]. To solve this problem, applying the remote sensing technology to measure

This work was supported in part by the National High-tech R&D Program of China (863 Program 2014AA06A503), the National Natural Science Foundation of China (61422307 and 61304048), the Scientific Research Starting Foundation for the Returned Overseas Chinese Scholars and Ministry of Education of China. Authors also gratefully acknowledge supports from the Youth Innovation Promotion Association, Chinese Academy of Sciences, the Youth Top-notch Talent Support Program, the 1000-talent Youth Program and the Youth Yangtze River Scholar. Zerui Li and Wenjun Lv are with Department of Automation, University of Science and Technology of China, Hefei, China. Yu Kang, corresponding author, is with Department of Automation and State Key Laboratory of Fire Science, University of Science and Technology of China, Hefei, China and with Key Laboratory of Technology in GeoSpatial Information Processing and Application System, Chinese Academy of Sciences, Beijing, China. Yunbo Zhao is with the College of Information Engineering, Zhejiang University of Technology, Hangzhou, China.

on-road vehicle emissions has been investigated in the last several decades, and has been successfully implemented in several major cities already, proving that it is an effective real-time method [3].

In 1998, Yu L. formed an on-road emission model to estimate relations of on-road vehicle emission rates and its instantaneous speed [4]. In 2006, Ko et al. measured fleet emissions using remote sensing technology in Taiwan. Their results revealed that different types of sampling sites has different vehicle emission levels. They also established an accurate quantitative relation of gas concentrations and mean speed or acceleration [5]. In China, Hong Kong has been at the forefront in the research of real-world vehicle emissions. The emission factors of CO, HC and nitric oxide (NO) of on-road vehicles fueled by petrol, diesel and liquefied petroleum gas were estimated using regression analysis to find the effects on emissions of instantaneous speed and acceleration profiles, respectively [6]–[8]. For China mainland, some mega-cities including Beijing, Shanghai, and Guangzhou, have paid much attention in studying vehicle emissions, which is unfortunately not popular in other smaller cities [9].

The experiments in this paper were carried out in Hefei, the provincial capital of Anhui. Unlike the fully developed mega-cities, Hefei is undergoing a phase of explosive growth, and consequently its vehicle population. It is reported that the total number of vehicles in Hefei has amounted to over 1.19 million by the end of 2014. Taking this reality into consideration, mobile assessment of emissions is more desirable in Hefei. In this work, we focus on light-duty gasoline vehicles, and two artificial neural networks (ANN) for each gaseous pollutant are established using the on-road emission data obtained with the aid of transportable vehicle emissions remote sensing system. Results presented in this paper support the use of the remote sensing system in motor vehicle emission measurements and offer help to the government to make strategies to improve the air quality in the future.

The rest of paper is organized as follows. Section 2 is devoted to the operating principles of the transportable vehicle emissions remote sensing system. Section 3 involves the construction of models and performance comparison of models we developed by using several statistical indices. The paper is concluded in Section 4.

## II. THE REMOTE ACQUISITION AND ANALYSIS OF ON-ROAD VEHICLE EMISSION DATA

The on-road emission data used in this work is acquired using a transportable vehicle emissions remote sensing system. In this section we describe the system and discuss several analysis issues of the data.

### A. Transportable vehicle emissions remote sensing system

Fig. 1 shows the diagram of the transportable vehicle emissions remote sensing system. This system can measure real-world vehicle emissions, i.e. CO, HC and NO, as well as the speed and acceleration of the vehicles. The system is composed of an exhaust detector, a speed/acceleration sensor, a video camera, an industrial controller and a transportable platform. The transportable system can be moved to any road to detect emissions of vehicles in the city due to its flexibility. In some sense it is a useful complementation of the fixed counterpart.



Fig. 1: Illustrating the transportable vehicle emissions remote sensing system.

The exhaust detector uses optical methods to measure emissions from vehicles as they are driven on the road, i.e., measuring concentrations of CO and HC by infrared absorption and NO by ultraviolet absorption. The gas concentrations in emissions from a single car can be determined according to the attenuation of beams in less than one second, expressed as volume percent in the exhaust. The speed/acceleration sensor measures vehicle speed and acceleration through measuring the interval between the passing of wheels with two optical gates. The video camera acquires an image of the passing vehicle and records its license information, which will be later used in order to determine vehicle-type information. The industrial controller is employed for managing other instruments and processing data. During the measurement, barricades are required to guide vehicles to pass through the transportable system. Finally, each vehicles emissions,

speed and acceleration are recorded and linked to other measurements, like time of measurement, weather, temperature, humidity, pressure, wind direction and wind speed, etc.

Because the amount of plume is affected by the wind and turbulence, we can only determine the ratios of CO, HC and NO, that is  $CO/CO_2$ ,  $HC/CO_2$  and  $NO/CO_2$ . For a given plume, these ratios are constant. In subsequent analysis, these ratios are converted to fuel-normalized emission rates [11]. Since each time of measurement only stands for a snapshot of the car's emissions, and vehicle emission level varies with time, in order to obtain the average estimation, a large number of vehicles have to be detected. Indeed, during the experiments, 38867 light-duty gasoline vehicles were recorded for further analysis.

### B. Data acquisition and preprocessing

The on-road emission data of massive vehicles was obtained from field measurements conducted in Hefei, Anhui province, China from May to August, 2012, making up a database containing 52745 records. After preprocessing, 42146 records were kept in the database as valid measurements, each of which embodies information about emissions, driving patterns and ambient meteorological conditions of an individual vehicle passing through the system. In existing studies, vehicles are usually divided into four types based on weight class (vehicles with weight less than  $3863kg$  is light-duty and greater than  $3863kg$  is heavy-duty) and engine type (gasoline or diesel fueled) [10]. Since the light-duty gasoline vehicles account for the majority of the total number of on-road vehicles, as for our experiments, 38867 records are of this type in the valid database, we focus on light-duty gasoline vehicle emissions.

The measurements were carried out during normal working hours in Hefei. Sampling locations were selected on roads with smooth traffic to capture a sufficient number of vehicles and a wide range of speeds and accelerations. In the database, the vehicle speed range has covered most of the urban driving speed profiles, with 4.3%, 62.6%, 31.2%, 1.5% and 0.4% of measured vehicles driven at the speed slower than 20, 20 to 40, 40 to 60, 60 to 80 and greater than 80 kilometers per hour respectively. The range of accelerations is within  $-10$  to  $10m/s^2$ .

Then exhaust concentrations by volume need to be converted to corresponding fuel-based emission factors expressed as grams of pollutant emitted per liter of fuel burnt. In order to finish this process, the conversion required, which has been incorporated into Holmen's research [13], can be formed as follows:

$$CO(gl^{-1}) = 1200 \frac{Q}{1 + Q + 3Q'/0.493}$$

$$HC(gl^{-1}) = 1800 \frac{Q'/0.493}{1 + Q + 3Q'/0.493}$$

$$NO(gl^{-1}) = 1293 \frac{Q''}{1 + Q + 3Q'/0.493}$$

For developing ANN models, data need to be scaled to a range suitable for the transfer function in ANNs. For a variable whose maximum and minimum values are denoted as  $x_{max}$  and  $x_{min}$ , respectively, each value  $x$  is scaled to  $x'$  according to the following equation:

$$x' = \frac{x - x_{min}}{x_{max} - x_{min}}$$

Before modelling, data are divided into three parts, that is, training, validation and testing sets. The training data set contains a sample of the different characteristics that may appear in the neural network models. The testing set can avoid overtraining through tracking errors during the training process. The validation set is used to evaluate the final models. A large training set can reduce the risk of undersampling but increases the training time. So an appropriate size of the training set should be chosen. In this study, the training set contains 50% of all the records. The testing and validation set contain 25% of the records, respectively.

### III. MODEL CONSTRUCTION AND RESULTS

It is studied that the instantaneous speed and the atmospheric turbulence of the plume have a significant influence on the vehicle emission concentrations measured by the remote sensing system [7]. It is therefore necessary to take driving patterns and meteorological conditions into account when estimating vehicle emissions. In this study, we choose the ANN technique to model the relationship between emissions and driving patterns and meteorological conditions. In the following, two ANNs, namely, the back-propagation (BP) neural network and radial basis function (RBF) neural network are employed to estimate the relations. A BP model and a RBF model are built for each pollutant (CO, HC and NO), and their performances are compared.

#### A. Model description

The information processing model, ANN is patterned after the biological neural network. It contains a series of mathematical equations for simulating biological processes like learning and memory [14]. The most widely used network topology is multiple layers with connections existing only between neurons of two adjacent layers, and neurons of the same layer have no connection [16]. The BP neural network and RBF neural network are among this type of topology.

##### a) Back-propagation (BP) neural network

The BP neural networks are the most prevalent and widely investigated neural network architecture. The BP networks are trained by recurring information forward-propagation and error back-propagation, which will be stopped until the error decreases to an acceptable value or a prespecified repetition number is achieved. During training, values of each weight and threshold are adjusted to make the deviation between expected output and real output minimum.

The activation function adopted in hidden neurons is the sigmoid function. It can be formed as follows,

$$g(x) = \frac{1}{1 + e^{-(x+\theta)}}$$

where  $\theta$  is the threshold value. The activation function is linear in the output layer.

The objective of BP neural network is to minimize

$$E = \frac{1}{2} \sum_k (t_k - o_k)^2$$

in which  $t_k$  and  $o_k$  are the predicted value and the actual value for the  $k$ th output neuron respectively.

##### b) Radial basis function (RBF) neural network

Similar to BP neural networks, RBF networks can approximate the nonlinear functions with several variables. The difference is that the radial basis function one has a "linear in the parameters" representation [18].

The RBF network is a feed-forward neural network with three layers. The hidden layer is composed of a set of radial basis functions, typical choice of which is the Gaussian function:

$$\alpha_i(x) = \exp \left[ \frac{-\|X - c_i\|^2}{2\sigma_i^2} \right], i = 1, 2, \dots, m$$

where  $\alpha_i(x)$  is the output of  $i$ th hidden neuron,  $X = (x_1, x_2, \dots, x_n)^T$ , is the inputs of the network,  $c_i$  and  $\sigma_i$  are the centre and width of the radial basis function at  $i$ th hidden neuron respectively,  $m$  is the number of hidden neurons. The training for the hidden layer is to select a centre for each neuron, instead of adjusting weight values. The output layer of a RBF network comprises a set of linear combiners.

Connection weights of output neurons can easily be computed using the least squares algorithm, by which the following learning algorithm is established:

$$w_{ik}(l+1) = w_{ik}(l) + \beta[y_k^d - y_k(l)]\alpha_i(x)/\alpha_i^T(x)$$

where  $y_k^d$  is the desired output,  $(l+1)$  is the  $(l+1)$ th iteration,  $\beta$  is the learning rate, whose value ranges from 0 to 2 to guarantee the convergence properties.

The successful establishment of neural network is dependent highly on its architecture, namely, the selection of number of layers and neurons in each layer. The number of neurons in the hidden layer, which cannot be specified only by the nature of the problem, should be paid attention to. For BP networks, a series of neural networks with different number of hidden neurons from 2 to 25 were tested, and then their performance was compared. Finally, the best one was selected. Through experiments, we chose the network architecture with 14, 18 and 13 for CO, HC and NO respectively. However for the RBF network, its training algorithm can increase the number of nodes in hidden layer repeatedly until the terminal condition is achieved.

#### B. Results and comparisons

This section will compare the estimation performance of developed models. After model development, all collected valid data can be input to the networks, and the outputs of each model are compared with the measurement data in Tab. I, where  $\bar{X}_{obs}$  and  $\bar{X}_{model}$  represent observed and estimated means.  $\sigma_{obs}$  and  $\sigma_{model}$  are standard deviations

of the measurement data and output data, whose calculation formulas are given as follows,

$$\sigma_{obs} = \sqrt{\frac{1}{n} \sum_{i=1}^n (X_{obs,i} - \overline{X_{obs}})^2}$$

$$\sigma_{model} = \sqrt{\frac{1}{n} \sum_{i=1}^n (X_{model,i} - \overline{X_{model}})^2}$$

where the subscripts *obs* and *model* represent the observed values and estimated values by ANN models, respectively. In a scatterplot of individual  $X_{obs,i}$  and  $X_{model,i}$  values, an intercept (*a*) 0.0 and a slope (*b*) 1.0 mean that the output exactly match observations [19]. The parameters *a* and *b* can be used for model performance evaluation. Details about measurement data and estimated data of neural networks are illustrated later in this paper.

From Tab. I, the estimated means of BP networks for CO and HC are larger than measurement means, but are the opposite for RBF networks. Both models under-estimate the emission factors of NO. Furthermore, the estimated means and standard deviations of BP networks for all three pollutants are larger than those of RBF networks. Comparing the proximity of *a* to 0 and *b* to 1, the estimated emission factors of CO are closest to measurement data, with *b* being 0.8132 and 0.8646 for BP and RBF models respectively.

In Tab. II, we conduct a comparison between different models by some indices, and took the multiple linear regression (MLR) approach as a reference to judge the performance of neural networks we developed. After establishing MLR models for three pollutants, their performance are summarized as well as that of six ANN models, assessed by mean absolute error (MAE), root mean square error (RMSE), mean relative deviation ( $\Delta$ ), correlation coefficient (R) and index of agreement (IA) as statistical indices of the fit level between actual and estimated fuel-based emission factors. These indices can be calculated in the following way:

$$MAE = \frac{1}{n} \sum_{i=1}^n |X_{obs,i} - X_{model,i}|$$

$$RMSE = \sqrt{\frac{1}{n} \sum_{i=1}^n (X_{obs,i} - X_{model,i})^2}$$

$$\Delta = \frac{1}{n} \sum_{i=1}^n \frac{X_{model,i} - X_{obs,i}}{X_{obs,i}}$$

$$R = \frac{\sum_{i=1}^n (X_{obs,i} - \overline{X_{obs}})(X_{model,i} - \overline{X_{model}})}{[\sum_{i=1}^n (X_{obs,i} - \overline{X_{obs}})^2 \cdot \sum_{i=1}^n (X_{model,i} - \overline{X_{model}})^2]^{\frac{1}{2}}}$$

$$IA = 1 - \frac{\sum_{i=1}^n (X_{model,i} - X_{obs,i})^2}{\sum_{i=1}^n (|X_{model,i} - \overline{X_{obs}}| + |X_{obs,i} - \overline{X_{obs}}|)^2}$$

From Tab. II, MAE of BP and RBF models for all three pollutants are smaller than that of MLR, and the values of either R or IA of both ANN models are larger than that of

MLR, which manifest the better performance of ANN models, and prove the effectiveness of ANN approach for estimating vehicle emission factors. It seems that BP models have a better stability for all pollutants, while RBF models obtain smaller values of MAE for CO and NO than BP models, and get smaller RMSE for CO and HC. It can be found that the finest value of R from BP models is 0.6122 for CO, and  $\Delta$  results about 1.4754 for HC, while RBF models obtain both the best R being 0.8820 and best  $\Delta$  being -0.0971 for CO, what's more, RBF networks obtain the best performance among all models for CO with largest IA being 0.9306. It should be noticed that the emission factors of CO are more related to the driving patterns and the meteorological conditions, for both ANN models for CO have larger values of R than that for other two pollutants and high values of IA.

From Tab. II, it is obvious that a single metric cannot evaluate model performance explicitly. By comparing several indices, it is observed that both ANN models perform better than MLR for any pollutant. Results show the usability of ANN to estimate emissions from mobile sources using meteorological conditions and driving patterns data. Performance of ANN models for CO, HC and NO are presented in detail in the following figures.

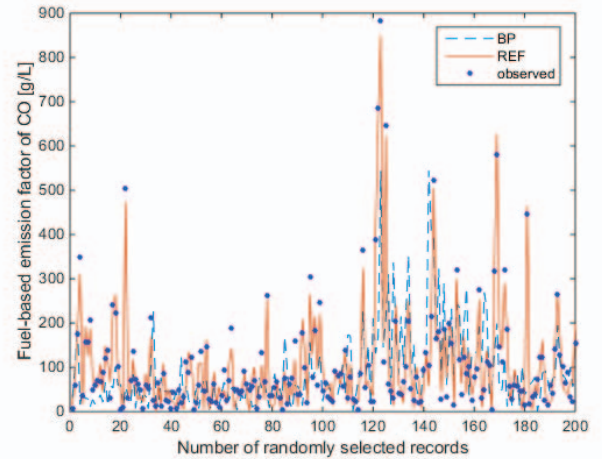


Fig. 2: BP and RBF performance for CO.

Fig. 2 to Fig. 4 show the comparison of actual values and estimated values of ANN models, with each figure corresponding to one of CO, HC and NO. For clarity of the description, 200 pieces of data from the total 38867 records are randomly chosen to be exhibited in the figures to analyse the performance of BP and RBF models.

In all the three figures, it can be noticed that RBF networks perform better than BP models for higher emission factors of CO, HC and NO, which may be caused by the fact that the objective function used in BP networks during training is apt to plunge into local minimum. In order to decrease the large error caused by higher emissions in the BP models, we can divide the total 33867 records into several subsets and establish BP models for each subsets. For instance, the total data can

TABLE I: Comparison between observed and estimated emission factors of CO, HC and NO

Model		$\overline{X_{obs}}$	$\overline{X_{model}}$	$\sigma_{obs}$	$\sigma_{model}$	<b>a</b>	<b>b</b>
CO	BP	87.1540	119.6682	93.9033	124.7389	48.7937	0.8132
	RBF	87.1540	68.4116	93.9033	92.0408	-6.9375	0.8646
HC	BP	1.1775	1.3801	1.8119	1.9089	0.6760	0.5979
	RBF	1.1775	0.8244	1.8119	1.1250	0.4292	0.3356
NO	BP	1.0281	0.9111	1.1154	0.8502	0.4449	0.4535
	RBF	1.0281	0.7636	1.1154	0.8409	0.2946	0.4561

TABLE II: Model performance

Model		MAE	RMSE	$\Delta$	<b>R</b>	<b>IA</b>
CO	BP	53.7706	105.3247	2.2827	0.6122	0.7447
	RBF	24.6666	48.9253	-0.0971	0.8820	0.9306
	MLR	58.2751	85.6589	1.0560	0.4097	0.5140
HC	BP	0.7404	1.7441	1.4754	0.5675	0.7497
	RBF	0.7751	1.5715	3.1294	0.5405	0.6882
	MLR	1.0948	1.6341	4.5600	0.4320	0.5291
NO	BP	0.5143	0.9232	3.1001	0.5950	0.7520
	RBF	0.4207	0.9414	1.7150	0.6051	0.7519
	MLR	0.7363	0.9850	4.2464	0.4436	0.5449

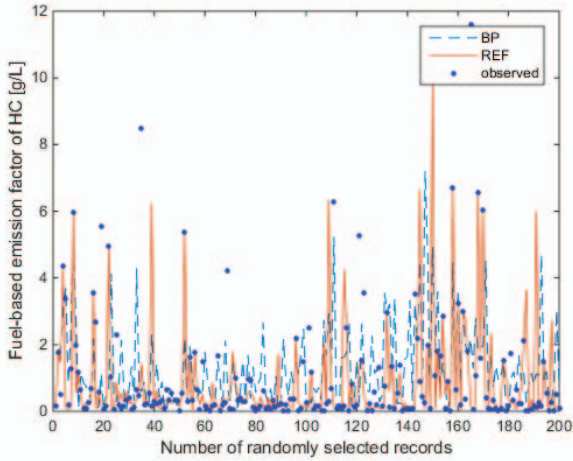


Fig. 3: BP and RBF performance for HC.

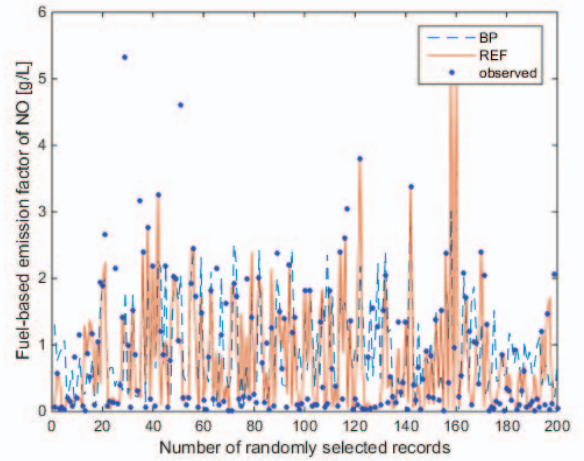


Fig. 4: BP and RBF performance for NO.

be separated into subsets with emission factors of CO less than  $200\text{gl}^{-1}$ ,  $200\text{gl}^{-1}$  to  $400\text{gl}^{-1}$ , and more than  $400\text{gl}^{-1}$  respectively. The first subset, which has been mentioned to account for 89.5% of the total number, is the subset with most records. Through calculating, the R of 0.6581 with RMSE 37.974 is obtained, which proves that BP performance is better without extreme values. As for the remaining two subsets,

new BP networks can be developed. Performance of BP model established using data from more-than- $400\text{gl}^{-1}$  subset, which includes records of high-emitted vehicles, is shown in Fig. 5. We also choose some of the more-than- $400\text{gl}^{-1}$  data randomly to be exhibited in the figure. It can be observed that the performance is also improved with the resulting value of R is 0.6563 and IA is 0.7809. Results show the effectiveness of

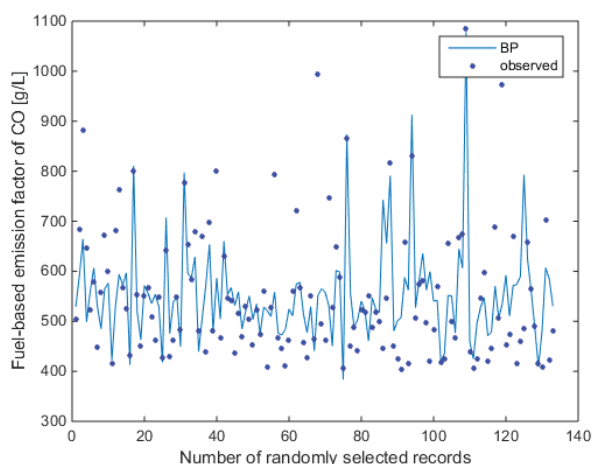


Fig. 5: BP performance for CO emission factors more than  $400\text{g/L}^{-1}$ .

the proposed design to improve performance of BP models.

Characteristics of high-emitted vehicles, namely the certain driving patterns and meteorological conditions, should be analyzed and summarized in the future studies provided that more information about vehicle types, model years, engine types etc. from the Vehicle Administrative Office can be combined with input parameters used in this paper. The knowledge acquired from established models verify that ANNs are suitable for emission factor evaluation, which can then be used for policy makers to formulate effective traffic control strategies to reduce pollution from mobile sources, improving environmental sustainability.

#### IV. CONCLUDING REMARKS

We used neural networks to estimate fuel-based emission factors of CO, HC and NO from vehicles measured by the transportable vehicle emissions remote sensing system using the influencing parameters, namely driving patterns and meteorological conditions. A BP network and a RBF network are developed for each pollutant. By comparing the results between them and also the MLR models, we show that neural networks give better performance than MLR models, and thus can be an effective tool to estimate fuel-based emission factors. These results provide a method to assess vehicle emissions based on the information of driving patterns and meteorological conditions, and assist relevant departments to make environmental plans to meet air quality standards.

One particular limitation of our present study is that the experiments were conducted in the spring and early summer, making the results possibly not suitable for winter conditions. This will be one of our future research directions.

#### REFERENCES

[1] V. Franco, *Evaluation and improvement of road vehicle pollutant emission factors based on instantaneous emissions data processing*, Tdx, 2014.

[2] M.D. Geller, S.B. Sardar, H.Phuleria, et al., *Measurements of particle number and mass concentrations and size distributions in a tunnel environment*, *Environmental Science & Technology*, vol. 39, no. 22, pp. 8653 - 8663, 2005.

[3] C. Mazzoleni, H. Moosmiller, H.D. Kuhns, et al., *Correlation between automotive CO, HC, NO, and PM emission factors from on-road remote sensing: implications for inspection and maintenance programs*, *Transportation Research Part D: Transport and Environment*, vol. 9, no. 6, pp. 477 - 496, 2004.

[4] L.Yu, *Remote vehicle exhaust emission sensing for traffic simulation and optimization models*, *Transportation Research Part D: Transport and Environment*, vol. 3, no. 5, pp. 337 - 347, 1998.

[5] Y.W. Ko, C.H. Cho, *Characterization of large fleets of vehicle exhaust emissions in middle Taiwan by remote sensing*, *Science of the total environment*, vol. 354, no. 1, pp. 75 - 82, 2006.

[6] T.L. Chan, Z. Ning, C.W. Leung, et al., *On-road remote sensing of petrol vehicle emissions measurement and emission factors estimation in Hong Kong*, *Atmospheric Environment*, vol. 38, no. 14, pp. 2055 - 2066, 2004.

[7] T.L. Chan and Z. Ning, *On-road remote sensing of diesel vehicle emissions measurement and emission factors estimation in Hong Kong*, *Atmospheric Environment*, vol. 39, no. 36, pp. 6843 - 6856, 2005.

[8] Z. Ning and T.L. Chan, *On-road remote sensing of liquefied petroleum gas (LPG) vehicle emissions measurement and emission factors estimation*, *Atmospheric Environment*, vol. 41, no. 39, pp. 9099 - 9110, 2007.

[9] H. Huo, Q. Zhang, K. He, et al., *Modeling vehicle emissions in different types of Chinese cities: importance of vehicle fleet and local features*, *Environmental Pollution*, vol. 159, no. 10, pp. 2954 - 2960, 2011.

[10] H.D. Kuhns, C. Mazzoleni, H. Moosmiller, et al., *Remote sensing of PM, NO, CO and HC emission factors for on-road gasoline and diesel engine vehicles in Las Vegas, NV*, *Science of the Total Environment*, vol. 322, no. 1, pp. 123 - 137, 2004.

[11] G.A. Bishop and D.H. Stedman, *Measuring the emissions of passing cars*, *Accounts of Chemical Research*, vol. 29, no. 10, pp. 489 - 495, 1996.

[12] B.C. Singer and R.A. Harley, *A fuel-based inventory of motor vehicle exhaust emissions in the Los Angeles area during summer 1997*, *Atmospheric Environment*, vol. 34, no. 11, pp. 1783 - 1795, 2000.

[13] B.A. Holmen and D.A. Niemeier, *Characterizing the effects of driver variability on real-world vehicle emissions*, *Transportation Research Part D: Transport and Environment*, vol. 3, no. 2, pp. 117 - 128, 1998.

[14] A.T.C. Goh, *Back-propagation neural networks for modeling complex systems*, *Artificial Intelligence in Engineering*, vol. 9, no. 3, pp. 143 - 151, 1995.

[15] J.V. Tu, *Advantages and disadvantages of using artificial neural networks versus logistic regression for predicting medical outcomes*, *Journal of clinical epidemiology*, vol. 49, no. 11, pp. 1225 - 1231, 1996.

[16] P.D. Heermann and N. Khazenie, *Classification of multispectral remote sensing data using a back-propagation neural network*, *Geoscience and Remote Sensing, IEEE Transactions on*, vol. 30, no. 1, pp. 81 - 88, 1992.

[17] C.P. Tsai and T.L. Lee, *Back-propagation neural network in tidal-level forecasting*, *Journal of Waterway, Port, Coastal, and Ocean Engineering*, vol. 125, no. 4, pp. 195 - 202, 1999.

[18] V.T. Elanayar and Y.C. Shin, *Radial basis function neural network for approximation and estimation of nonlinear stochastic dynamic systems*, *Neural Networks, IEEE Transactions on*, vol. 5, no. 4, pp. 594 - 603, 1994.

[19] C.J. Willmott, *On the validation of models*, *Physical geography*, vol. 2, no. 2, pp. 184 - 194, 1981.

## 1. Remote sensing and artificial neural network estimation of on-road vehicle emissions

**Accession number:** 20164903084982

**Authors:** Li, Zerui (1); Kang, Yu (1); Lv, Wenjun (1); Zhao, Yunbo (2)

**Author affiliation:** (1) Department of Automation, University of Science and Technology of China, Hefei; 230022, China; (2) College of Information Engineering, Zhejiang University of Technology, Hangzhou; 310023, China

**Source title:** ICARM 2016 - 2016 International Conference on Advanced Robotics and Mechatronics

**Abbreviated source title:** ICARM - Int. Conf. Adv. Robotics Mechatronics

**Issue title:** ICARM 2016 - 2016 International Conference on Advanced Robotics and Mechatronics

**Issue date:** October 21, 2016

**Publication year:** 2016

**Pages:** 561-566

**Article number:** 7606982

**Language:** English

**ISBN-13:** 9781509033645

**Document type:** Conference article (CA)

**Conference name:** 2016 International Conference on Advanced Robotics and Mechatronics, ICARM 2016

**Conference date:** August 18, 2016 - August 20, 2016

**Conference location:** Macau, China

**Conference code:** 124470

**Sponsor:** IEEE Control System Society (Beijing Chapter); IEEE Robotics and Automation Society (Guangdong Chapter); IEEE Systems, Man and Cybernetics Society; South China University of Technology; University of Macau

**Publisher:** Institute of Electrical and Electronics Engineers Inc.

**Abstract:** The emissions of on-road vehicles are studied based on a remote sensing system and artificial neural network models. A transportable vehicle emission remote sensing system is used to collect the emission data from May to August 2012 in Hefei, China. Based on these light-duty gasoline vehicle data containing the emission pollutants such as carbon monoxide, hydrocarbons, nitric oxide, and so on, artificial neural network models are constructed to estimate the relation of fuel-based emission factors and input parameters. The performance of the developed models is analyzed and compared, showing that neural networks perform better than the multiple linear regression models, thus validating the effectiveness of neural networks in vehicle emission estimation. © 2016 IEEE.

**Number of references:** 19

**Main heading:** Remote sensing

**Controlled terms:** Carbon - Carbon monoxide - Linear regression - Neural networks - Nitric oxide - Regression analysis - Robotics - Vehicles

**Uncontrolled terms:** Artificial neural network models - Developed model - Emission factors - Light duty gasoline vehicles - Multiple linear regression models - On-road vehicle emissions - Remote sensing system - Vehicle emission

**Classification code:** 731.5 Robotics - 804 Chemical Products Generally - 804.2 Inorganic Compounds - 922.2 Mathematical Statistics

**DOI:** 10.1109/ICARM.2016.7606982

**Funding Details: Acronym; Sponsor:** CAS; Chinese Academy of Sciences - **Number; Acronym; Sponsor:** 61304048; NSFC; National Natural Science Foundation of China - **Number; Acronym; Sponsor:** 61422307; NSFC; National Natural Science Foundation of China - **Acronym; Sponsor:** ZJUT; Zhejiang University of Technology

**Compendex references:** YES

**Database:** Compendex

Compilation and indexing terms, Copyright 2017 Elsevier Inc.

**Data Provider:** Engineering Village